nature neuroscience

Hepatocyte growth factor mediates mesenchymal stem cell–induced recovery in multiple sclerosis models

Lianhua Bai[1], Donald P Lennon[2], Arnold I Caplan[2], Anne DeChant[1], Jordan Hecker[1], Janet Kranso[1], Anita Zaremba[1] & Robert H Miller[1]

Mesenchymal stem cells (MSCs) have emerged as a potential therapy for a range of neural insults. In animal models of multiple sclerosis, an autoimmune disease that targets oligodendrocytes and myelin, treatment with human MSCs results in functional improvement that reflects both modulation of the immune response and myelin repair. Here we demonstrate that conditioned medium from human MSCs (MSC-CM) reduces functional deficits in mouse $MOG_{35–55}$-induced experimental autoimmune encephalomyelitis (EAE) and promotes the development of oligodendrocytes and neurons. Functional assays identified hepatocyte growth factor (HGF) and its primary receptor cMet as critical in MSC-stimulated recovery in EAE, neural cell development and remyelination. Active MSC-CM contained HGF, and exogenously supplied HGF promoted recovery in EAE, whereas cMet and antibodies to HGF blocked the functional recovery mediated by HGF and MSC-CM. Systemic treatment with HGF markedly accelerated remyelination in lysolecithin-induced rat dorsal spinal cord lesions and in slice cultures. Together these data strongly implicate HGF in mediating MSC-stimulated functional recovery in animal models of multiple sclerosis.

Multiple sclerosis is an autoimmune disease that results in progressive functional deficits. The initial course of the disease is characterized by relapsing and remitting episodes that frequently progress to a more chronic functional loss[1]. The target of immunological attack appears to be myelin sheaths, and the loss of myelin and death of myelinating oligodendrocytes leaves axons functionally compromised and vulnerable to damage[2]. Most therapies for multiple sclerosis are directed toward suppression of the immune response; however, long-term functional recovery is likely to depend on the ability of the CNS to replace lost oligodendrocytes and repair myelin sheaths damaged by disease. The realization that the adult CNS retains a population of oligodendrocyte precursors[3], as well as more multipotent neural stem cells[4], has encouraged the development of therapies oriented toward myelin repair.

The use of animal models such as EAE have facilitated the development of new therapeutic approaches for multiple sclerosis, as well as our understanding of the pathobiology of demyelinating diseases. Induction of EAE by immunization with peptides of myelin oligodendrocyte glycoprotein (MOG) results in chronic functional deficits that are correlated with areas of demyelination and inflammation in white matter tracts, particularly in the spinal cord. Likewise, the use of local chemically induced demyelination such as that resulting from the injection of lysolecithin (LPC) or ethidium bromide has illuminated the details of myelin repair.

Cell-based therapies are emerging as an important approach to the treatment of multiple sclerosis[5,6]. Whereas most therapies are directed toward modulation of the immune system, cell-based therapies offer the possibility of localized multifaceted influences that promote effective remyelination during the course of the disease concomitant with modulation of immunological attack[6]. Several stem cell populations have shown therapeutic promise in the setting of different neural insults. For example, neural stem cells promote repair in models of multiple sclerosis[5,7], and adult oligodendrocyte progenitors identified by expression of the proteoglycan NG2 ($NG2^+$ cells) enhance axonal regeneration after spinal cord injury[8]. One of the most intensively studied stem cell populations in the context of tissue regeneration is MSCs[9]. Initial work identified MSCs as a powerful regulator of graft-versus-host disease (GVHD) after bone marrow stem cell transplants[10], and more recently they are emerging as a promising approach for cell-based therapies for several neurological disorders, including stroke[11], spinal cord injury[12], multiple sclerosis[6,13,14] and other demyelinating diseases[15].

In animal models of multiple sclerosis, the efficacy of MSCs at enhancing functional recovery appears to reflect their ability to modulate both the immune system and neural cell responses[13,16]. In EAE, treatment with MSCs results in a biasing of the immune response from pro-inflammatory T_H1-based to anti-inflammatory T_H2-based responses[13]. In addition, MSCs localize to the areas of demyelination in the CNS and promote functional recovery. Although MSCs have been proposed to have the capacity to give rise to neural cells[17] in the setting of demyelination, their primary function appears to be the promotion of endogenous repair mechanisms[13] that we show can be recapitulated by conditioned medium, suggesting it reflects the release of soluble factors.

The molecular mechanisms responsible for functional recovery in EAE following treatment with MSCs have not been identified. Here we show that the effects of MSCs reside in a fraction of

[1]Center for Translational Neuroscience, Department of Neurosciences, Case School of Medicine, Case Western Reserve University, Cleveland, Ohio USA. [2]Skeletal Research Center, Case Western Reserve University, Cleveland, Ohio, USA. Correspondence should be addressed to R.H.M. (rhm3@case.edu).

Received 18 January; accepted 17 April; published online 20 May 2012; doi:10.1038/nn.3109

MSC-conditioned medium a critical component of which is HGF. HGF is a pleiotropic cytokine made primarily by cells of mesenchymal origin. Originally described as a mitogen for hepatocytes[18], HGF has been identified in many different tissues, including the CNS[19]. In general, HGF is thought to promote angiogenesis and cell survival[20,21], and injection of HGF has been demonstrated to enhance kidney and liver regeneration, as well as protect against the onset of renal failure[22]. The effects of HGF are not restricted to liver and kidney, and it has been shown to prolong the survival of cardiac allografts and improve myocardial function after myocardial infarction[23].

The biological effects of HGF are primarily mediated by the tyrosine kinase transmembrane receptor cMet[24]. During development, cMet is expressed in several different tissues, including the CNS[25] and liver. Expression in liver is retained in normal adult and activated during parenchymal regeneration in adult mice[26], consistent with a role for this pathway in tissue regeneration.

In this study we identify a central role for the HGF-cMet signaling pathway in mediating functional recovery and remyelination stimulated by MSCs. Human MSCs in growth conditions secrete HGF, and their capacity to promote recovery in EAE depends on signaling through the cMet receptor. The beneficial effects of both MSC-CM and HGF in EAE are selectively blocked by treatment with function-blocking cMet and with antibodies to HGF (anti-HGF). Systemic treatment with HGF markedly accelerates the rate of remyelination in a non–immune-mediated spinal cord LPC lesion model of demyelination and in cerebellum slice cultures. These data support the notion that a major role of MSCs is to provide a source of trophic factors[14], including HGF, that modulate the inflammatory environment in demyelinating diseases and stimulate endogenous neural cell remyelination to enhance functional recovery.

RESULTS

MSC-CM modulates neural development and disease in EAE

Long-term functional recovery in demyelinating disease depends on myelin repair and suppression of pathogenesis, both of which appear to be influenced by MSCs. To determine whether the neural responses and functional recovery seen after treatment of animals infused with MSCs reflect release of soluble factors, we assayed the effects of MSC-conditioned medium (MSC-CM) on neural cell development and functional recovery. Exposure of neurosphere cultures to MSC-CM resulted in a reduction in the proportion of astrocytes and an increase in the proportion of antibody A2B5$^+$ oligodendrocyte precursor cells (OPCs), oligodendrocytes and neurons that developed (**Fig. 1a**). In control cultures after 3 d *in vitro*, approximately 30% of cells were glial fibrillary acidic protein (GFAP)-positive astrocytes and A2B5$^+$ OPCs, 25% were O4$^+$ immature oligodendrocytes and less than 5% neurons. By contrast, after 72 h in MSC-CM, the proportion of astrocytes was reduced to 20%, and the proportion of O4$^+$ cells (50%) and neurons (25%) increased significantly (**Fig. 1b**; $P < 0.05$).

Injection of MSC-CM rapidly reduced the disease load in EAE mice (**Fig. 1c**). Injection of MSC-CM 17 d after $MOG_{35–55}$ immunization, at the peak of disease, resulted in a rapid reduction in functional deficits in 11 of 11 mice. Whereas control mice maintained a clinical score between 2.5 and 3, where 0 is unaffected and 5 is dead or moribund, all mice that received MSC-CM showed some functional improvement. Four of the 11 mice improved to a clinical score of 1 and two other mice appeared completely normal within 5 d. This functional recovery was correlated with a reduction in the extent of regions of demyelination seen in spinal cord sections stained with luxol fast blue (**Fig. 1d**).

MSC-CM stimulated recovery depends on a 50–100-kDa activity

Size fractionation studies demonstrated that the disease-modifying activity of MSC-CM required a fraction with a molecular mass between 50 and 100 kDa. Fractions with masses 1–50 kDa did not significantly modify disease progression in $MOG_{35–55}$ EAE *in vivo* (data not shown). By contrast, 1–100-kDa (MSC-CM_{100kDa}) fractions reduced disease burden in the EAE model ($n = 11$) (**Fig. 2a**) and increased the proportion of oligodendrocytes and neurons from neurosphere cultures (**Fig. 2b**). This functional improvement was correlated with improvements in the histology of the spinal cord that were comparable to those seen with complete MSC-CM. Injection of unconditioned control medium or heat-inactivated MSC-CM ($n = 8$) had no obvious effect on either functional outcome or histology.

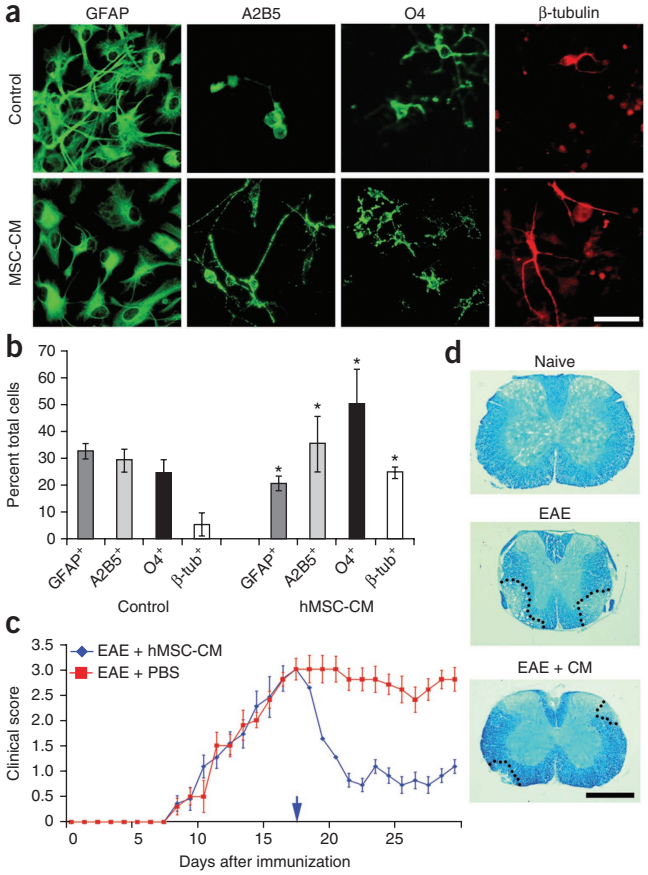

Figure 1 Conditioned growth medium from human MSCs biases the development of neurosphere derived cells toward oligodendrocytes and neurons, and promotes functional recovery in $MOG_{35–55}$-induced EAE. (**a**) In the presence of human MSC-CM, the proportion or GFAP$^+$ astrocytes is reduced and the proportion of oligodendrocyte-lineage cells and neurons is increased. (**b**) Quantitation of cell types in the presence and absence of MSC-CM. *Control versus MSC-CM: A2B5 $P < 0.01$, O4 $P < 0.05$, β-tubulin (β-tub) $P < 0.05$, GFAP $P = 0.005$. Mean ± s.e.m. of duplicate preparations taken from three independent experiments. Note there are both overlapping expression and unlabeled cells in these preparations. (**c**) Treatment with MSC-CM (0.5 mg) (arrow), but not PBS, at peak of disease after $MOG_{35–55}$ immunization results in functional improvement in EAE. Mean ± s.e.m. of all mice, $n = 11$. (**d**) The functional improvement is correlated with a reduction in myelin loss and tissue damage seen with luxol fast blue staining of spinal cord sections; lesions are outlined. Scale bars: 50 μm in **a**, 500 μm in **d**.

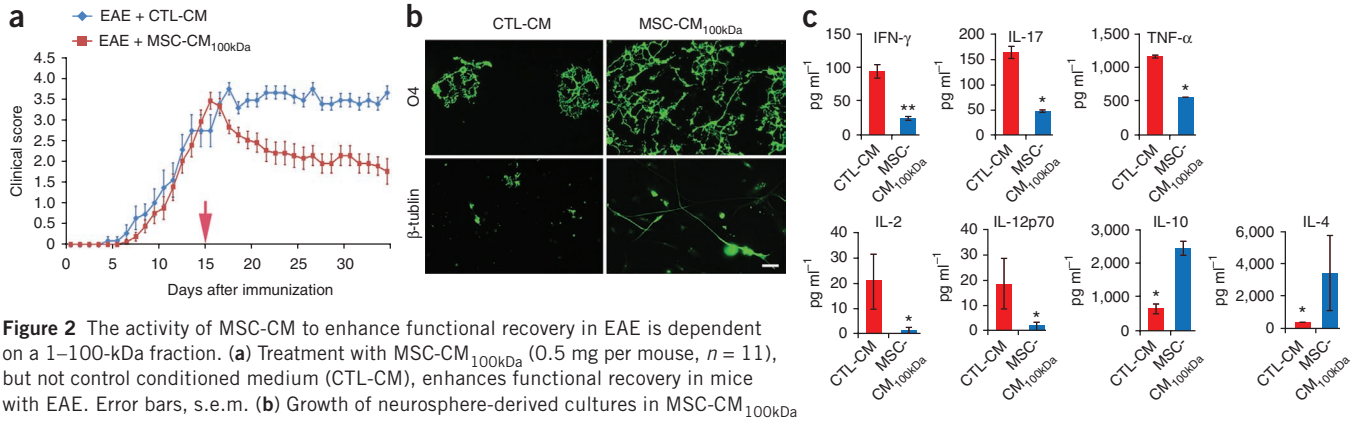

Figure 2 The activity of MSC-CM to enhance functional recovery in EAE is dependent on a 1–100-kDa fraction. (**a**) Treatment with MSC-CM$_{100kDa}$ (0.5 mg per mouse, $n = 11$), but not control conditioned medium (CTL-CM), enhances functional recovery in mice with EAE. Error bars, s.e.m. (**b**) Growth of neurosphere-derived cultures in MSC-CM$_{100kDa}$ biases cell development in favor of oligodendrocytes and neurons compared to growth in CTL-CM. (**c**) Treatment with MSC-CM$_{100kDa}$ reduces proinflammatory cytokine expression by spinal cord–derived mononuclear cells in EAE mice. Significantly reduced expression of IFN-γ, IL-17, TNF-α, IL-2 and IL-12p70 and increased expression of IL-10 and IL-4 were seen in mice treated with MSC-CM$_{100kDa}$. $^*P = 0.05$, $^{**}P = 0.01$. Mean ± s.e.m. from three independent experiments.

Isolation of mononuclear cells from the spinal cords of control and MSC-CM$_{100kDa}$-treated EAE mice demonstrated alterations in the relative levels of inflammatory cytokines (**Fig. 2c**). At day 35 after EAE onset, the level of the proinflammatory cytokines interferon-γ (IFN-γ), interleukin (IL)-17, tumor necrosis factor-α (TNF-α), IL-2 and IL-12p70 were decreased in mice that received MSC-CM$_{100kDa}$, whereas levels of anti-inflammatory cytokines such as IL-10 and IL-4 were increased.

Recombinant HGF modulates disease progression in EAE

On the basis of the size fractionation studies, known MSC expression data[27,28] and previously described biological properties[29,30], we identified HGF as a candidate molecule in the MSC-CM$_{100kDa}$ fraction that could modulate disease in EAE. Western blot analyses of active MSC-CM$_{100kDa}$ identified HGF (molecular mass, 62 kDa α chain + 34 kDa β chain) at a concentration of between 600 and 800 ng ml^{-1} in all active samples ($n = 6$) but not in unconditioned control medium (**Fig. 3a**). To determine whether recombinant HGF treatment could promote functional recovery in EAE, mice at the peak of disease (clinical score = 3) received injections of either PBS ($n = 10$) or HGF at two different concentrations (50 and 100 ng per mouse, $n = 10$ each) every other day over a 5-d period (days 1, 3 and 5) and their clinical scores were monitored for 30 d after immunization. The clinical scores of control

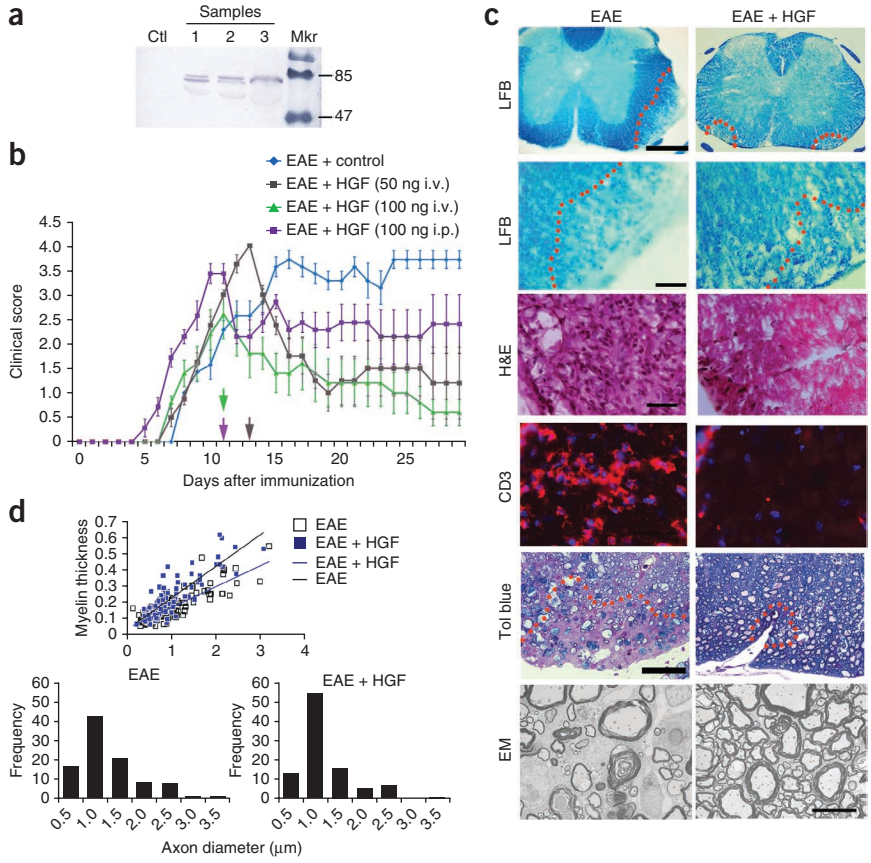

Figure 3 Human MSC-CM$_{100kDa}$ contains HGF and HGF promotes functional and histological recovery in EAE. (**a**) Western blot of three samples of active MSC-CM$_{100kDa}$ shows the presence of HGF. Ctl, unconditioned control medium; Mkr, size marker (kDa). (**b**) Treatment with HGF (one injection every other day for a total of three over a 5-d period, $n = 10$) results in functional improvement compared to vehicle control treatment. Arrows indicate treatment initiation day. Error bars, s.e.m. (**c**) HGF improves tissue histology. Sections after 100 ng i.v. at 30 d after immunization with MOG$_{35–55}$. The improvement in myelination is apparent by luxol fast blue (LFB) staining. The reduction in immune cell infiltrates is evident in hematoxylin and eosin (H&E) and anti-CD3-labeled sections and confirmed in toluidine blue (tol blue)-stained 1-μm sections. EM, representative electron micrographs through spinal cord lesion areas in EAE control and HGF-treated mice 17 d after initiation of treatment. Outlines define lesion area. (**d**) Top: analysis of myelin thickness versus axon diameter in lesion areas of control and HGF-treated mice demonstrates thicker myelin in HGF-treated animals compared to controls. Bottom: comparison of the relative axon diameters in lesion areas of control EAE and HGF-treated mice demonstrates a reduction in small-diameter fibers and an increase in medium-diameter fibers in HGF-treated animals. Scale bars: 500 μm in **c** LFB (top); 50 μm in **c** LFB (second panel), H&E, CD3 and toluidine blue; 2 μm in EM.

mice remained relatively constant between 3–3.5, whereas mice that received HGF improved (**Fig. 3b**). The higher dose of HGF appeared to provide slightly better functional recovery, although both doses reduced the mean functional score below 1.5 (**Fig. 3b**). The functional improvement after intraperitoneal (i.p.) injection of HGF (100 ng) was less than that after i.v. injection. For example, at 30 d after immunization the mean score of i.p.-treated mice was approximately 2.4, as compared to 1.5 for i.v. treated animals (**Fig. 3b**). All subsequent studies used i.v. delivery.

The HGF-induced functional improvement was closely correlated with histological improvement. In control EAE mice, luxol fast blue staining revealed extensive regions of white matter pathology along the length of the spinal cord 30 d after immunization (**Fig. 3c**). In HGF-treated mice at the same stage, the degree of demyelination was markedly reduced and most white matter appeared relatively normal (**Fig. 3c**). Inflammatory cell infiltration in EAE mice was also reduced in HGF-treated animals. In control EAE mice, hematoxylin and eosin staining revealed white matter regions with a high density of infiltrated cells (**Fig. 3c**), and labeling with antibodies to CD3 confirmed this (**Fig. 3c**). Both the extent of the infiltrate and the density of cells were reduced in mice treated with HGF. Myelin integrity was confirmed in 1-μm Epon resin sections labeled with toluidine blue and by ultrastructural analyses (**Fig. 3c**) that demonstrated a decrease in the number of unmyelinated axons. In lesion areas of EAE mice a majority of axons were unmyelinated (80 ± 20%), whereas in lesion areas of HGF-treated EAE mice a minority (10 ± 4% $P = 0.05$) were unmyelinated. Analyses of myelin thickness in lesion areas showed that HGF treatment resulted in substantially thicker myelin sheaths

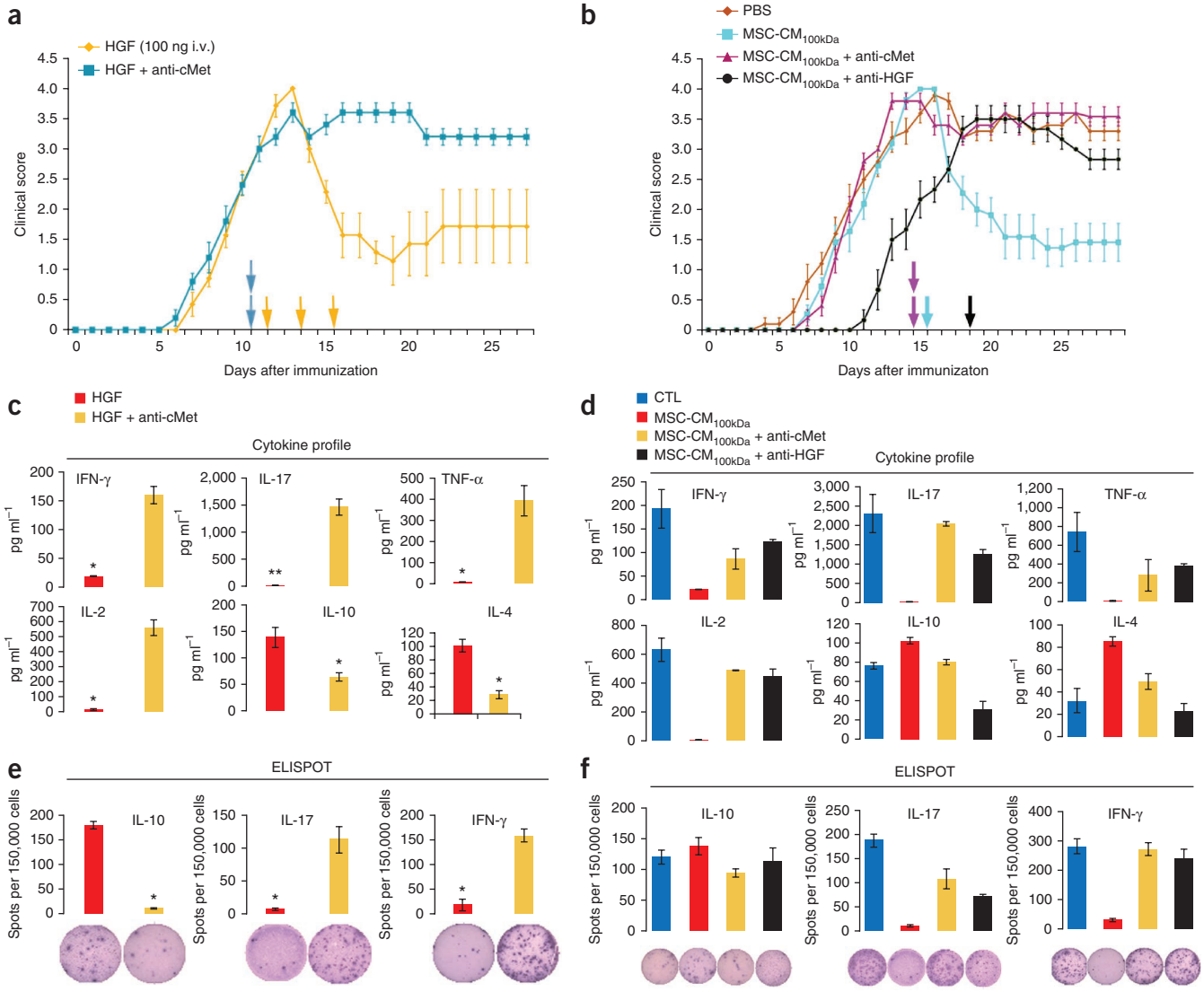

Figure 4 Inhibition of HGF signaling with cMet antibodies negates the capacity of both HGF and MSC-CM to induce functional recovery and reverses EAE-induced changes in cytokine expression. (**a**) Two injections of function-blocking cMet antibodies 12 h apart (blue arrows), delivered 1 d before initiation of HFG treatment regimen (yellow arrows) inhibits functional recovery. (**b**) Similarly, cMet inhibition blocks MSC-CM_{100kD}-stimulated functional recovery. Two injections of function-blocking cMet antibody (purple arrows) at peak of disease or anti-HGF (black arrow) inhibits recovery. (**c**,**d**) Treatment with cMet antibodies increases proinflammatory cytokine expression and reduces anti-inflammatory cytokine expression as shown by cytokine profile in mice treated with HGF (**c**) or MSC-CM_{100kDa} (**d**). (**e**,**f**) ELISPOT analysis on spinal cord–derived cells demonstrates that treatment with cMet antibodies increases the frequencies of T_H1 and T_H17 cells compared to those in mice treated with HGF alone (**e**) or MSC-CM_{100kDa} alone (**f**). The delay in disease onset reflects the use of a different preparation of $MOG_{35–55}$ peptide and not anti-HGF treatment. The data are representative from triplicate studies; ELISPOT counts represent the mean ± s.d. from one of three experiments. $*P = 0.05$, $**P = 0.01$; error bars, s.d.

around small-diameter axons, as well as an increase in the relative number of small-diameter (<1 μm) axons (**Fig. 3d**). Together these studies suggest that treatment of EAE mice with HGF results in substantial functional improvement and an enhancement in the extent of spinal cord remyelination.

To examine the timing of HGF-induced histological improvement, we assessed histology of mice on 1-μm sections at the time of treatment initiation and 3, 11 and 17 d thereafter. Spinal cords had extensive demyelinated lesions and cellular infiltrates at initiation of treatment that were still apparent after 3 d of treatment (**Supplementary Fig. 1**). After a further 8 d, the lesions were largely resolved, although there was a residual elevated cellularity. By 17 d after initiation of treatment, light microscopy (**Fig. 3c**) and ultrastructural analyses (**Fig. 3c**) revealed extensive remyelination in HGF-treated mice, with essentially all fibers, including small-diameter fibers, extensively myelinated. These data suggest HGF both reduces pathological pressure and enhances or facilitates myelin repair.

HGF- and MSC-CM–stimulated recovery is mediated by cMet

In other systems the biological properties of HGF are mediated through the tyrosine receptor kinase cMet, the best characterized receptor for HGF[31]. To determine whether the functional benefits of HGF in EAE were also mediated by cMet, we treated EAE mice with a function-blocking cMet antibody[32,33] (250 ng twice per mouse i.v., 24 h before HGF treatment). In mice that received control immunoglobulin G followed by three injections of HGF at the peak of disease (n = 8), functional improvements were evident after 24 h that plateaued after 5–7 d (**Fig. 4a**). By contrast, mice treated with cMet antibodies (n = 10) did not show any substantial improvement over the subsequent 14 d. Histologically the lesions in mice treated with

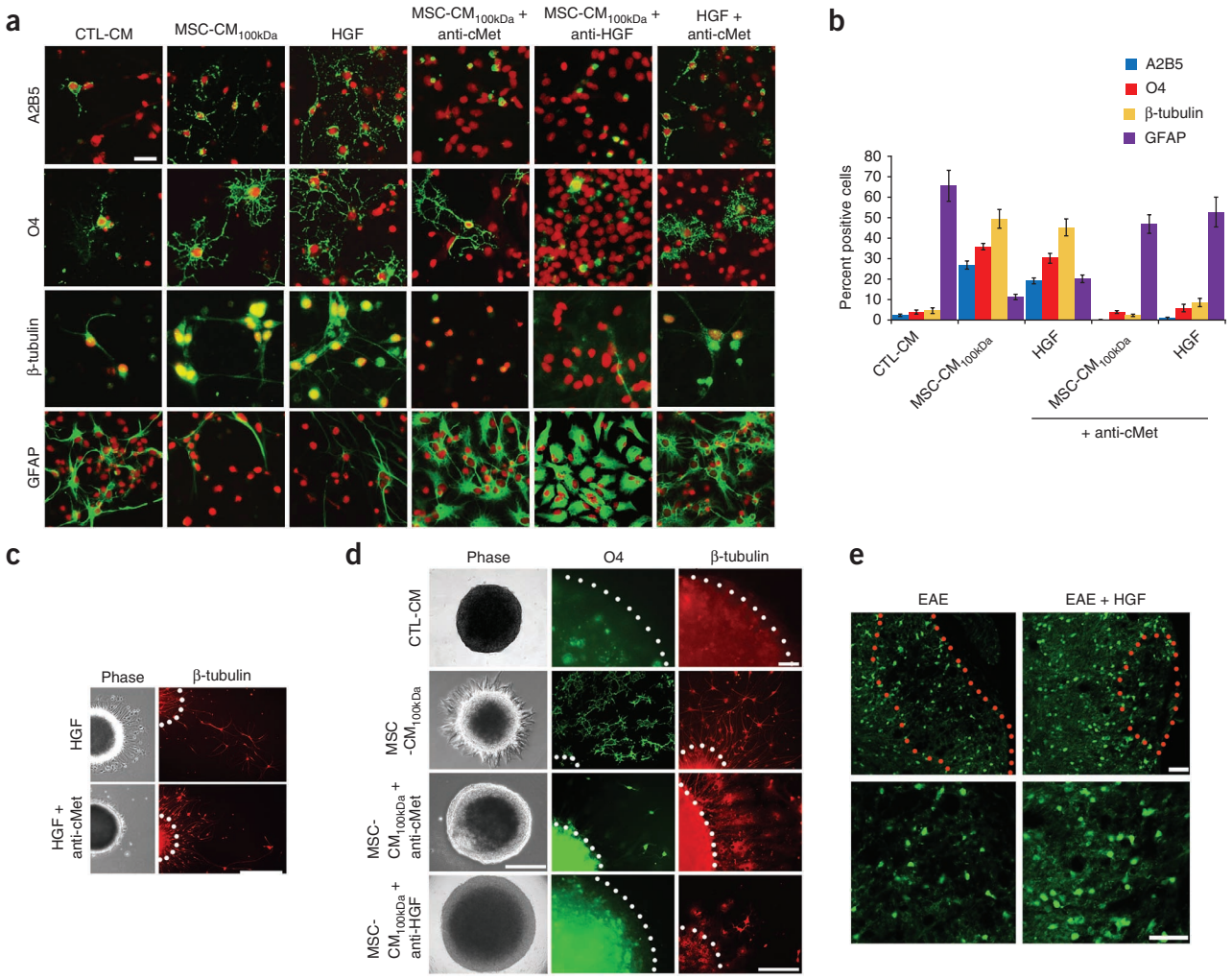

Figure 5 Inhibition of HGF signaling with cMet or anti-HGF blocks the ability of MSC-CM$_{100kDa}$ and HGF to alter the development and migration of neural cells from neurospheres. (**a**) The proportions of A2B5$^+$, O4$^+$, β-tubulin$^+$ and GFAP$^+$ cells are altered in the presence of MSC-CM$_{100kDa}$ and HGF, and reversed by cMet and anti-HGF. (**b**) Quantification of cell types in the presence and absence of MSC-CM$_{100kDa}$ and HGF, with or without cMet antibodies. Compared to that in controls, the proportion of O4$^+$ and β-tubulin$^+$ cells is increased by MSC-CM and HGF (P < 0.05 for both), and this increase is blocked by cMet antibodies (P < 0.01 for both). Mean ± s.d. of the proportion of individual cell types taken from five random fields from at least two independent experiments. Note that there are both unlabeled cells and overlap of antigen expression on individual cells. (**c**) Treatment with HGF stimulates migration of neuronal precursors from adult SVZ-derived neurospheres of EAE mice, and this effect is blocked by anti-cMet. (**d**) Treatment with MSC-CM$_{100kDa}$ stimulates migration of OPCs and neuronal precursors from adult EAE SVZ-derived neurospheres, and this effect is blocked by cMet and anti-HGF. (**e**) The mobilization of PLP$^+$ OPCs into EAE lesions is enhanced in mice treated with HGF. The number of EGFP-PLP cells that populate lesions increases upon HGF treatment. Outlining defines neurosphere edges. Scale bars: 20 μm in **a**, 100 μm in **c**,**d**. 50 μm in **e**. Lesion areas are outlined in **e**.

cMet antibodies appeared similar to those in controls that did not receive HGF, with only limited remyelination (data not shown).

Treatment with cMet antibodies also negated the capacity of HGF to modulate the immune response in EAE mice (**Fig. 4**). For example, compared to levels in untreated EAE mice, we detected relatively low levels of the proinflammatory cytokines IFN-γ, IL-17, TNF-α, and IL-2 in HGF-treated animals, and these were elevated in those that received cMet antibodies (**Fig. 4c**). Likewise, the levels of anti-inflammatory cytokines IL-10 and IL-4, elevated in HGF-treated mice, were reduced after treatment with cMet antibodies (**Fig. 4c**). Enzyme-linked immunosorbent spot (ELISPOT) assays demonstrated that HGF treatment resulted in a reduction in the frequency of spinal cord–derived $MOG_{35–55}$-specific proinflammatory cytokine (IFN-γ, IL-17)-producing cells and an increase in IL-10–producing cells that was reversed by cMet antibody treatment (**Fig. 4e**). These results confirm that, in the setting of EAE, the biological activity of HGF is mediated through cMet.

Treatment with cMet antibodies blocked MSC-CM-mediated functional recovery. In control immunoglobulin G–treated mice (two injections, 24 h before treatment), MSC-CM stimulated a rapid and sustained functional recovery (**Fig. 4b**) (n = 9). By contrast, mice treated with cMet antibodies showed little or no functional improvement over the subsequent 15 d (**Fig. 4b**) (n = 11). Treatment of MSC-CM with function-blocking anti-HGF for 2 h before injection also inhibited its capacity to reduce functional deficits in EAE (**Fig. 4b**). Cytokine analyses revealed that the decrease in proinflammatory cytokines and the increase in anti-inflammatory cytokines associated with MSC-CM were largely reversed by prior treatment with cMet antibodies (**Fig. 4d**), as were the alterations in the frequencies of antigen-specific IFN-γ-, IL-17- and IL-10–secreting cells shown by ELISPOT analysis (**Fig. 4f**). These data strongly suggest that HGF signaling in MSC-CM is critical for mediating functional recovery and promoting histological improvement in MOG-induced EAE.

cMet mediates HGF/MSC-CM stimulation of neural development

To assess the role of HGF in $MSC\text{-}CM_{100kDa}$-induced neural cell development, we compared HGF and $MSC\text{-}CM_{100kDa}$ treatment as to their relative generation of the different classes of neural cells from postnatal neurospheres and the dependence on cMet signaling. In control neurosphere-derived cultures grown for 7 d, the proportion of $A2B5^+$ OPCs, $O4^+$ oligodendrocyte lineage cells and β-tubulin$^+$ neurons was below 10%, and the proportion of $GFAP^+$ astrocytes was greater than 60% (**Fig. 5a**,**b**). By contrast, in the presence of $MSC\text{-}CM_{100kDa}$ the proportion of $A2B5^+$ OPCs was increased to approximately 25%, the proportion of $O4^+$ cells was greater than 30% and the proportion of β-tubulin$^+$ neurons was greater than 40%, whereas the proportion of astrocytes was markedly reduced (to ~10%). In both cases, cells tended to form clusters, although this was more prevalent in controls, and total cell numbers were not significantly different in either condition. Similar changes in cell proportions were seen in cultures treated with HGF (45 ng per 3×10^5 cells), although the reduction in $GFAP^+$ astrocytes was less pronounced with HGF than with $MSC\text{-}CM_{100kDa}$. Blocking cMet negated the effects of both $MSC\text{-}CM_{100kDa}$ and HGF, and the cellular composition of the cultures reverted to that of controls (**Fig. 5a**,**b**). Similarly, incubation of $MSC\text{-}CM_{100kDa}$ with function-blocking anti-HGF negated

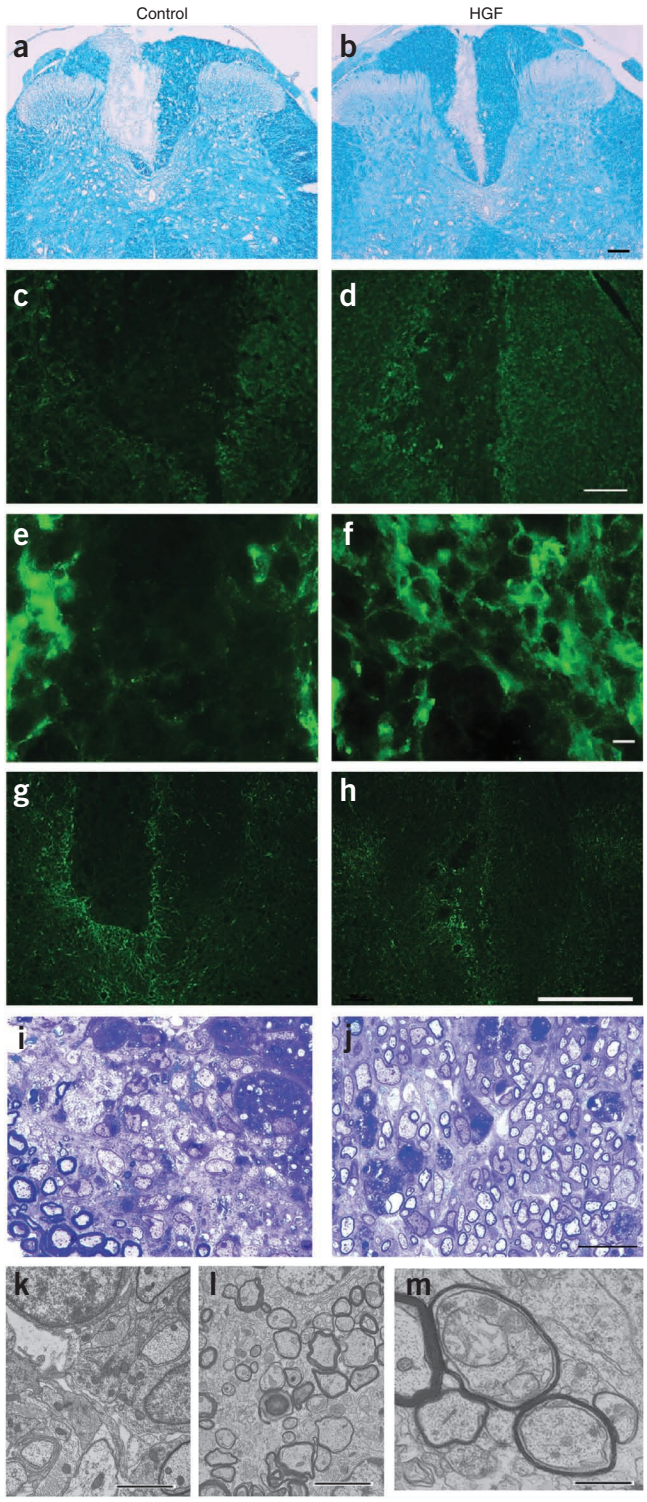

Figure 6 Systemic HGF treatment stimulates remyelination of rat spinal cord LPC lesions. (**a**,**b**) Treatment with 0.8 mg kg^{-1} HGF 5, 9 and 11 dpl results in smaller demyelinated lesions at 14 dpl as shown by luxol fast blue. (**c**–**h**) Immunohistochemical labeling of frozen sections, demonstrating an increase in MBP labeling (**c**,**d**), increase in $NG2^+$ cells (**e**,**f**) and a decrease in GFAP expression (**g**,**h**) in lesion areas from HGF-treated rats 14 dpl. (**i**,**j**) Toluidine blue sections 1 μm thick show extensive remyelination at 14 dpl in HGF-treated rats but not in controls, and ultrastructural analyses shows that axons of different caliber have myelin sheaths of different thicknesses, indicative of ongoing repair, in HGF (**l**,**m**) but not control lesions (**k**). (**m**) G ratios showing thin myelin sheaths in HGF-treated rats. Scale bars: **a**–**f**, 100 μm; **g**,**h**, 50 μm; **i**,**j**, 5 μm; **k**, 1 μm; **l**, 2 μm; **m**, 0.5 μm.

its effects on neural cell development, consistent with a major role for MSC-CM-derived HGF in the regulation of neural cell development (**Fig. 5a**,**b**).

Repopulation of demyelinated lesions depends on OPCs migration, which can be stimulated by MSCs[34]. To assess whether EAE pathology responses were dependent on cMet, we established neurospheres from the subventricular zones of mice with ongoing EAE and compared cell migration in the presence or absence of MSC-CM_{100kDa} or HGF with or without cMet-supplemented medium. Cell migration was enhanced in the presence of HGF, and this was inhibited by cMet antibodies (**Fig. 5c**). Similarly, cell migration from EAE-derived neurospheres was enhanced by MSC-CM_{100kDa}, and this effect was blocked by anti-cMet or anti-HGF (**Fig. 5d**). Most migratory cells gave rise to either neurons (**Fig. 5c**,**d**) or oligodendrocytes (**Fig. 5d**), and very few generated astrocytes (data not shown). Consistent with HGF mobilizing OPCs and enhancing remyelination, *in vivo* EAE lesions of mice treated with HGF contained more than twice as many oligodendrocyte lineage cells identified by expression of the reporter EGFP from the proteolipid protein promoter (EGFP-PLP) (3.1 ± 0.3 per 200 μm^2) than lesions of control mice (1.8 ± 0.2 per 200 μm^2) (**Fig. 5e**). The average number of lesions was also significantly reduced in mice treated with HGF compared to controls. Control EAE mice had 6 ± 0.4 areas of lesion in an average section, and this was reduced to 3.4 ± 0.6 in those treated with HGF ($P < 0.05$).

HGF promotes repair in non–immune-mediated demyelination

The restitution of histological integrity seen in EAE upon treatment with HGF is likely a combination of suppression of the immune response and the promotion of myelin repair. To determine whether HGF promotes myelin repair in non–immune-mediated demyelination *in vivo*, we used a spinal cord LPC lesion and slice culture model. In rats injected i.v. with HGF (0.8 μg per kilogram body weight) on days 4, 6 and 11 after an LPC lesion and examined on 14 or 28 days post-lesion (dpl), we saw a 30% reduction in overall lesion volume by luxol fast blue staining compared to that in saline controls (**Fig. 6a**,**b**). Labeling of frozen sections with antibodies to myelin basic protein (MBP) demonstrated only limited expression in control lesions, whereas in the HGF-treated lesions we saw substantial MBP staining throughout the lesion 14 dpl (**Fig. 6c**,**d**). Similarly, the density of $NG2^+$ cells was increased approximately eightfold in HGF-treated lesions (4 ± 2 to 33 ± 5 per cm^2; $P < 0.005$) (**Fig. 6e**,**f**,) and more than 25% of these cells were proliferating as shown by Ki67 double labeling (data not shown). By contrast, whereas control lesions showed an extensive astrocyte response, with intense GFAP labeling around the lesion perimeter, this was substantially attenuated in HGF-treated rats (**Fig. 6g**,**h**).

The increase in NG2 and MBP labeling in the HGF-treated lesions was accompanied by a marked increase in the extent of remyelination (**Fig. 6i**–**m**). In control lesions ($n = 9$), few myelinated axons were present in lesions, even at the lesion edge (**Fig. 6i**), whereas in HGF-treated rats ($n = 8$) myelinated axons were distributed throughout the lesion, interspersed with cells full of myelin debris (**Fig. 6j**). Ultrastructural analyses showed that control lesions contained largely unmyelinated axons, some of which were ensheathed in glial processes (**Fig. 6k**), whereas in HGF-treated rats, lesions contained axons of different sizes at different stages of remyelination, some with relatively thick myelin sheaths (**Fig. 6l**) but most with thin myelin (**Fig. 6m**). Calculation of the relative thickness of the myelin sheath to axon diameter (G ratio) confirmed the abundance of thinly myelinated axons in HGF-treated lesions (**Fig. 6n**) and showed a greater than fivefold increase in the density of remyelinated axons (from 18 ± 2 to 130 ± 6 per cm^2; $P < 0.0002$). Treatment with 0.4 μg ml^{-1} HGF resulted in increased but less profound enhancement of remyelination, and by 28 dpl some limited remyelination was apparent in controls although the beneficial effects of HGF were still evident (data not shown).

Consistent with the HGF-induced functional recovery in LPC lesions, treatment of LPC-demyelinated slice cultures with HGF enhanced recovery. Slices of postnatal day 7 cerebellum myelinated extensively *in vitro* over a 7-d period (**Supplementary Fig. 2a**), and treatment with LPC induced a rapid and sustained demyelination (**Supplementary Fig. 2a**). Exposure of LPC-treated slices to 50 ng ml^{-1} HGF promoted re-ensheathment by oligodendrocytes and reestablished the cytoarchitecture of the slice (**Supplementary Fig. 2a**). A lower dose of HGF (10 ng ml^{-1}) had little effect, whereas a higher dose (90 ng ml^{-1}) resulted in marginal additional improvement. A similar HGF-induced recovery of MBP profiles was seen in slice cultures from cerebral cortex treated with HGF (**Supplementary Fig. 2a**). Quantification of the extent of myelination of individual oligodendrocytes demonstrated a 2.5-fold decrease after LPC treatment that was largely reversed by HGF treatment (**Supplementary Fig. 2b**). This HGF induced functional recovery was negated by exposure to anti-cMet (**Supplementary Fig. 2b**). This recovery likely reflects stimulation of oligodendrocyte development, as addition of 50 ng ml^{-1} HGF to dissociated cell cultures from postnatal day 0 spinal cord increased the proportion of $O4^+$ and $O1^+$ cells, from approximately 3% ($O4^+$) and 1% ($O1^+$) in control cultures to greater than 15% ($O4^+$) and 23% ($O1^+$) after 3 d in HGF (**Supplementary Fig. 2c**,**d**). To confirm the expression of cMet on OPCs, we double-labeled cells with A2B5 and anti-cMet *in vitro* after 3 d in culture. Virtually all OPCs in culture expressed cMet (**Supplementary Fig. 3a**–**c**). By contrast, *in vivo* in naive rats very few cells of the oligodendrocyte lineage expressed detectable cMet, whereas in the setting of demyelinating lesions virtually all cells of the oligodendrocyte lineage expressed high levels of cMet (**Supplementary Fig. 3d**–**f**).

Taken together, these studies suggest that the ability of MSCs to reduce disease burden in models of EAE is dependent on their promotion of HGF signaling that both regulates immunomodulation and enhances remyelination in the setting of demyelinating disease.

DISCUSSION

Recent studies suggest that stem cell–based approaches are promising therapies for the treatment of demyelinating diseases such as multiple sclerosis. Mesenchymal stem cells have emerged as an attractive candidate for the treatment of neurological pathologies on the basis of their effectiveness, relative accessibility, ease of expansion and expression of trophic factors[9]. Previous studies indicated that bone marrow–derived MSCs promoted functional recovery and reduced lesion load in animal models of EAE[6,13,35], and these observations have led to the development of several clinical trials using MSCs for the treatment of multiple sclerosis[36].

Here we show that in EAE, an animal model of multiple sclerosis, human MSC growth-conditioned medium is effective at promoting functional recovery through a combination of immune suppression and promotion of myelination. Several lines of evidence indicate that these MSC activities depend on the secretion of hepatocyte growth factor (HGF). For example, fractionation studies indicate the activity of MSC-CM mediating functional recovery in EAE is contained in a 50–100-kDa fraction, consistent with HGF with a molecular mass of approximately 62–65 kDa for the α and 34 kDa for the β chain[37]. Treatment of mice after the onset of EAE disease with HGF reduced the severity of disease, and pretreatment with cMet antibodies blocked the effects of both HGF and MSC-CM, while pretreatment with anti-HGF blocked the effects of MSC-CM. The cellular responses to MSC-CM and HGF were similar.

Both stimulated the development and migration of oligodendrocytes and neurons and reduced the emergence of astrocytes from neurosphere cultures. Likewise, both MSC-CM and HGF reduced proinflammatory cytokine expression and enhanced anti-inflammatory cytokine expression, and HGF markedly enhanced remyelination in LPC-induced spinal cord demyelination and promoted ensheathment following demyelination in slice cultures of cerebellum and cortex.

The observations that HGF is required for MSC-CM-mediated functional recovery in EAE is consistent with the observations that MSCs release a variety of growth factors[9] including HGF and that this can be enhanced by stimulation with epidermal growth factor or TNF-α[28]. In many different conditions the biological effects of MSCs and HGF are similar. For example, in GVHD, a major complication that follows transplantation of allogeneic bone marrow, MSCs provide robust benefit, reducing the incidence of GVHD[38], and in a mouse model of GVHD, transfection of human HGF into skeletal muscle was found to inhibit damage to the gut and liver and enhance survival[39]. Similarly, MSCs appear to show promise for the treatment of myocardial infarcts, and transfection of HGF directly into the myocardium in a mouse model of autoimmune myocarditis reduced disease burden through a reduction in cardiomyocyte apoptosis and through induction of T_H2 anti-inflammatory cytokines[40]. Finally, a recent study demonstrated that mice in which expression of HGF was driven from a neuronal specific promoter were resistant to EAE owing to tolerization of dendritic cells and induction of T_H2 cytokines[41], consistent with previous studies using MSC treatments in EAE[13,42].

Mesenchymal stem cells and HGF influence similar cellular targets in both the CNS and immune system. In the CNS, HGF is expressed both during development and in the adult, where it has been suggested to act as a neurotrophic factor[19]. Consistent with this hypothesis, cMet is expressed on a range of neuronal populations[19], and cMet stimulation promotes axon outgrowth and neuronal differentiation in many neuronal populations[29]. The expression of cMet and the effects of HGF are not restricted to neurons. Astrocytes, microglia and oligodendrocyte precursors have been shown to express cMet[30,43]. The expression of cMet on oligodendrocyte lineage cells appears to be environmentally regulated. Whereas most OPCs are $cMet^+$ *in vitro* and in lesions of the CNS, they are $cMet^-$ in naive tissue. In humans the expression of cMet is less well characterized, but it has been described on some CNS tumor cells and microglia[8,43]. Which of these cellular targets are critical for the myelin repair seen in HGF- or MSC-CM-treated animals is unknown. Likewise, in the immune system, dendritic cells express cMet, and HGF induces tolerance in this cell population[41]. Both MSC-CM and HGF bias T cells away from T_H1 and toward T_H2 responses, as well as regulating the expression of IL-10 (ref. 41). The relative contributions of HGF-mediated modulation of immune response and local stimulation of myelin repair are unclear. However, the rapid, widespread remyelination of spinal cord LPC lesions seen after HGF treatment suggests that HGF promotes myelin repair in the absence of modulating the immune system. For example, although LPC injection does induce an immune response, it results in a rapid but brief influx of immune cells between 6 and 48 h (ref. 44). In the current studies, we delayed treatment with HGF until 5 dpl, a time when the lesion has mostly developed. In general, remyelination follows recruitment of OPCs to the lesion area and occurs over a 3- to 5-week period[45]. By contrast, in HGF-treated rats robust remyelination was apparent throughout the lesion by 14 dpl and only 9 d after the commencement of treatment. This rapid repair suggests that HGF both recruits OPCs and enhances remyelination.

The beneficial effects of transient HGF treatment are sustained in EAE. The reduced EAE disease burden in mice that constitutively express HGF from the neuron-specific enolase promoter may reflect the continuous expression of elevated HGF. In the current studies, however, a series of three injections of HGF at the peak of disease resulted in functional and histological recovery that was sustained for up to 2 weeks, the longest time examined. Although HGF is known to pass across the blood brain barrier[46], given that its half-life is thought to be relatively short after injection[46], the mechanisms that result in this long-term benefit are unclear. It may be that a short period of stimulated recovery is sufficient to inhibit further pathogenesis by permanently shifting the balance of pathological pressure and in favor of repair[47]. Alternatively, in other systems it has been demonstrated that elevation of exogenous HGF results in sustained elevation of endogenous HGF through a proposed positive feedback auto loop[48]. Finally, the effect of HGF may be to alter the balance of pro- and anti-inflammatory T cells in EAE on a long-term basis, possibly by influencing dendritic cell secretion of IL-23. If such a mechanism were operative, it could explain persistent recovery.

A function for HGF in multiple sclerosis has not been defined. Previous studies suggest that in patients with multiple sclerosis, as well as those with other neurological diseases, the HGF is elevated in cerebrospinal fluid. Although this has been proposed to correlate with pathology, particularly demyelinating pathology, our studies suggest it is more likely a reflection of an endogenous repair process stimulated by the disease. Indeed, it may be that susceptibility or disease progression in multiple sclerosis is, in part, a reflection of the capacity of endogenous MSCs to release HGF. Consistent with this hypothesis, *Hgf* gene expression decreases with age in mouse MSCs, and although MSCs from patients with multiple sclerosis have similar proliferative, differentiative and cell surface properties to control MSCs, they differ in their cytokine profiles.

In conclusion, we show that the therapeutic efficacy of MSCs in EAE is a result of secreted signals that are found in growth-conditioned medium. The biological effects of the conditioned medium depend on the presence of HGF, and sustained functional recovery in EAE follows a transient treatment with exogenously supplied HGF. The effects of both HGF and MSC-CM are mediated through the tyrosine kinase receptor cMet and include enhanced myelin repair as well as immunomodulation. These studies raise the possibility that the HGF-cMet pathway may provide new therapeutic opportunities for the treatment of multiple sclerosis.

METHODS

Methods and any associated references are available in the online version of the paper.

Note: Supplementary information is available in the online version of the paper.

ACKNOWLEDGMENTS

We thank M. Hitomi for electron microscopy support, D. Carrino for help with fractionation, S. Miller for microfluidics and A. Kerstetter for help with cell culture. This study was supported by the Myelin Repair Foundation and US National Institutes of Health grant NS 30800 (R.H.M.) and the Virginia and David Baldwin Fund (A.I.C., D.P.L.).

AUTHOR CONTRIBUTIONS

L.B., A.I.C. and R.H.M. conceived the study and experimental design. D.P.L. and A.I.C. prepared and processed the mesenchymal stem cells. L.B. performed all EAE experiments, immunohistochemistry and data analysis. A.Z. designed and conducted the slice and culture studies. J.H. and J.K. conducted the LPC lesion studies. L.B., A.I.C., A.D. and R.H.M. wrote the paper and designed the figures. All authors discussed the results and implications and commented on the manuscript at all stages.

COMPETING FINANCIAL INTERESTS

The authors declare no competing financial interests.

Published online at http://www.nature.com/doifinder/10.1038/nn.3109.
Reprints and permissions information is available online at http://www.nature.com/reprints/index.html.

1. Prineas, J.W. The neuropathology of multiple sclerosis. in *Handbook of Clinical Neurology* (ed. Koestier, J.C.) 15–30 (Elsevier, Amsterdam, 1985).
2. Trapp, B.D. *et al.* Axonal transection in the lesions of multiple sclerosis. *N. Engl. J. Med.* **338**, 278–285 (1998).
3. Wolswijk, G. & Noble, M. Identification of an adult-specific glial progenitor cell. *Development* **105**, 387–400 (1989).
4. Reynolds, B.A. & Weiss, S. Generation of neurons and astrocytes from isolated cells of the adult mammalian central nervous system. *Science* **255**, 1707–1710 (1992).
5. Ben-Hur, T. & Goldman, S.A. Prospects of cell therapy for disorders of myelin. *Ann. NY Acad. Sci.* **1142**, 218–249 (2008).
6. Uccelli, A., Pistoia, V. & Moretta, L. Mesenchymal stem cells: a new strategy for immunosuppression? *Trends Immunol.* **28**, 219–226 (2007).
7. Pluchino, S. *et al.* Injection of adult neurospheres induces recovery in a chronic model of multiple sclerosis. *Nature* **422**, 688–694 (2003).
8. Busch, S.A. *et al.* Adult NG2+ cells are permissive to neurite outgrowth and stabilize sensory axons during macrophage-induced axonal dieback after spinal cord injury. *J. Neurosci.* **30**, 255–265 (2010).
9. Caplan, A.I. & Dennis, J.E. Mesenchymal stem cell as trophic mediators. *J. Cell Biochem.* **98**, 1076–1084 (2006).
10. Lazarus, H.M. *et al.* Cotransplantation of HLA-identical sibling culture-expanded mesenchymal stem cells and hematopoietic stem cells in hematologic malignancy patients. *Biol. Blood Marrow Transplant.* **11**, 389–398 (2005).
11. Yoo, S.W. *et al.* Mesenchymal stem cells promote proliferation of endogenous neural stem cells and survival of newborn cells in a rat stroke model. *Exp. Mol. Med.* **40**, 387–397 (2008).
12. Jung, D.I. *et al.* A comparison of autologous and allogenic bone marrow-derived mesenchymal stem cell transplantation in canine spinal cord injury. *J. Neurol. Sci.* **285**, 67–77 (2009).
13. Bai, L. *et al.* Human bone marrow-derived mesenchymal stem cell induce Th2 polarized immune response and promote endogenous repair in animal models of multiple sclerosis. *Glia* **57**, 1192–1203 (2009).
14. Rafei, M., Birman, E., Forner, K. & Galipeau, J. Allogeneic mesenchymal stem cells for treatment of experimental autoimmune encephalomyelitis. *Mol. Ther.* **17**, 1799–1803 (2009).
15. Tanaka, F. *et al.* Exogenous administration of mesenchymal stem cells ameliorates dextran sulfate sodium-induced colitis via anti-inflammatory action in damaged tissue in rats. *Life Sci.* **83**, 771–779 (2008).
16. Barhum, Y. *et al.* Intracerebroventricular transplantation of human mesenchymal stem cells induced to secrete neurotrophic factors attenuates clinical symptoms in a mouse model of multiple sclerosis. *J. Mol. Neurosci.* **41**, 129–137 (2010).
17. Krampera, M. *et al.* Induction of neural-like differentiation in human mesenchymal stem cells derived from bone marrow, fat, spleen and thymus. *Bone* **40**, 382–390 (2007).
18. Michalopoulos, G.K. Liver regeneration: molecular mechanisms of growth control. *FASEB J.* **4**, 176–187 (1990).
19. Achim, C.L. *et al.* Expression of HGF and cMet in the developing and adult brain. *Brain Res. Dev. Brain Res.* **102**, 299–303 (1997).
20. Sulpice, E. *et al.* Cross-talk between the VEGF-A and HGF signalling pathways in endothelial cells. *Biol. Cell* **101**, 525–539 (2009).
21. Kitamura, K. *et al.* Hepatocyte growth factor promotes endogenous repair and functional recovery after spinal cord injury. *J. Neurosci. Res.* **85**, 2332–2342 (2007).
22. Anan, F. *et al.* Predictors for silent cerebral infarction in patients with chronic renal failure undergoing hemodialysis. *Metabolism* **56**, 593–598 (2007).
23. Deuse, T. *et al.* Hepatocyte growth factor or vascular endothelial growth factor gene transfer maximizes mesenchymal stem cell-based myocardial salvage after acute myocardial infarction. *Circulation* **120**, S247–S254 (2009).
24. Sheth, P.R., Hays, J.L., Elferink, L.A. & Watowich, S.J. Biochemical basis for the functional switch that regulates hepatocyte growth factor receptor tyrosine kinase activation. *Biochemistry* **47**, 4028–4038 (2008).
25. Sonnenberg, E., Meyer, D., Weidner, K.M. & Birchmeier, C. Scatter factor/hepatocyte growth factor and its receptor, the c-met tyrosine kinase, can mediate a signal exchange between mesenchyme and epithelia during mouse development. *J. Cell Biol.* **123**, 223–235 (1993).
26. Ishiki, Y., Ohnishi, H., Muto, Y., Matsumoto, K. & Nakamura, T. Direct evidence that hepatocyte growth factor is a hepatotrophic factor for liver regeneration and has a potent antihepatitis effect *in vivo*. *Hepatology* **16**, 1227–1235 (1992).
27. Polisetti, N. *et al.* Gene expression profile of epithelial cells and mesenchymal cells derived from limbal explant culture. *Mol. Vis.* **16**, 1227–1240 (2010).
28. Wang, Y. *et al.* MEK, p38, and PI-3K mediate cross talk between EGFR and TNFR in enhancing hepatocyte growth factor production from human mesenchymal stem cells. *Am. J. Physiol. Cell Physiol.* **297**, C1284–C1293 (2009).
29. Ebens, A. *et al.* Hepatocyte growth factor/scatter factor is an axonal chemoattractant and a neurotrophic factor for spinal motor neurons. *Neuron* **17**, 1157–1172 (1996).
30. Yan, H. & Rivkees, S.A. Hepatocyte growth factor stimulates the proliferation and migration of oligodendrocyte precursor cells. *J. Neurosci. Res.* **69**, 597–606 (2002).
31. Bottaro, D.P. *et al.* Identification of the hepatocyte growth factor receptor as the c-met proto-oncogene product. *Science* **251**, 802–804 (1991).
32. Sun, W., Funakoshi, H. & Nakamura, T. Localization and functional role of hepatocyte growth factor (HGF) and its receptor c-met in the rat developing cerebral cortex. *Brain Res. Mol. Brain Res.* **103**, 36–48 (2002).
33. van der Horst, E.H. *et al.* Discovery of fully human anti-MET monoclonal antibodies with antitumor activity against colon cancer tumor models *in vivo*. *Neoplasia* **11**, 355–364 (2009).
34. Bai, L., Caplan, A., Lennon, D. & Miller, R.H. Mesenchymal stem cell signals regulate neural stem cell fate. *Neurochem. Res.* **32**, 353–362 (2007).
35. Gerdoni, E. *et al.* Mesenchymal stem cells effectively modulate pathogenic immune response in experimental autoimmune encephalomyelitis. *Ann. Neurol.* **61**, 219–227 (2007).
36. Siatskas, C., Payne, N.L., Short, M.A. & Bernard, C.C. A consensus statement addressing mesenchymal stem cell transplantation for multiple sclerosis: it's time!. *Stem Cell Rev.* **4**, 500–506 (2010).
37. Birchmeier, C. & Gherardi, E. Developmental roles of HGF/SF and its receptor, the c-Met tyrosine kinase. *Trends Cell Biol.* **8**, 404–410 (1998).
38. Koç, O.N. *et al.* Allogeneic mesenchymal stem cell infusion for treatment of metachromatic leukodystrophy (MLD) and Hurler syndrome (MPS-IH). *Bone Marrow Transplant.* **30**, 215–222 (2002).
39. Kuroiwa, T. *et al.* Hepatocyte growth factor ameliorates acute graft-versus-host disease and promotes hematopoietic function. *J. Clin. Invest.* **107**, 1365–1373 (2001).
40. Futamatsu, H. *et al.* Hepatocyte growth factor ameliorates the progression of experimental autoimmune myocarditis: a potential role for induction of T helper 2 cytokines. *Circ. Res.* **96**, 823–830 (2005).
41. Benkhoucha, M. *et al.* Hepatocyte growth factor inhibits CNS autoimmunity by inducing tolerogenic dendritic cells and CD25+Foxp3+ regulatory T cells. *Proc. Natl. Acad. Sci. USA* **107**, 6424–6429 (2010).
42. Karussis, D. & Kassis, I. The potential use of stem cells in multiple sclerosis: an overview of the preclinical experience. *Clin. Neurol. Neurosurg.* **110**, 889–896 (2008).
43. Di Renzo, M.F. *et al.* Selective expression of the Met/HGF receptor in human central nervous system microglia. *Oncogene* **8**, 219–222 (1993).
44. Ghasemlou, N., Jeong, S.Y., Lacroix, S. & David, S. T cells contribute to lysophosphatidylcholine-induced macrophage activation and demyelination in the CNS. *Glia* **55**, 294–302 (2007).
45. Franklin, R.J. & Ffrench-Constant, C. Remyelination in the CNS: from biology to therapy. *Nat. Rev. Neurosci.* **9**, 839–855 (2008).
46. Pan, W. *et al.* Permeation of hepatocyte growth factor across the blood-brain barrier. *Exp. Neurol.* **201**, 99–104 (2006).
47. Miller, R.H. & Fyffe-Maricich, S.L. Restoring the balance between disease and repair in multiple sclerosis: insights from mouse models. *Dis. Model. Mech.* **3**, 535–539 (2010).
48. Hayashi, S. *et al.* Autocrine-paracrine effects of overexpression of hepatocyte growth factor gene on growth of endothelial cells. *Biochem. Biophys. Res. Commun.* **220**, 539–545 (1996).

ONLINE METHODS

Immunization. All studies were approved by Case Western Reserve University School of Medicine's IACUC, and animals were maintained in a NIH/AAALAC-approved facility. Chronic EAE was induced in 8- to 12-week-old female C57BL/6 mice (200) by subcutaneous immunization with 200 µl of 200 µg $MOG_{35–55}$ with complete Freund's adjuvant. Pertussis toxin (500 ng) (List Biological Laboratories, Campbell, CA) was injected i.p. at 0 and 2 d. Animals were sacrificed at day 35 by transcardial perfusion with 4% paraformaldehyde. Animals were graded according to a standard clinical index: 1 = limp tail; 2 = hind limb weakness; 3 = plegia of one limb; 4 = plegia of two limbs; 5 = moribund or dead.

Induction of local demyelination and HGF treatment. LPC-induced demyelination of the spinal cord was performed as described previously[49]. Animals (24) were anesthetized with 0.001 ml per kg of body weight of 3 ml ketamine (100 mg/ml) (Fort Dodge), 3 ml xylazine (20 mg/ml) (Lloyd Laboratories), 1 ml acepromazine (10 mg/ml) (Webster Vet). A T10 laminectomy was performed and 1.5 µl of 1% freshly prepared LPC (Sigma) solution was infused at 15 ml h^{-1}. Rats received either 0.4 or 0.8 µg/kg HGF or vehicle control on days 5, 6 and 11 by tail vein injection. Animals were sacrificed at day 14 or 28.

Preparation of human mesenchymal stem cells conditioned medium and treatment protocols. Human MSCs were isolated from bone marrow aspirates and grown in low-glucose DMEM supplemented with 10% FBS. This growth medium was collected between days 11 and 14 (MSC-CM). The MSCs used to prepare conditioned medium were derived from five separate donors to insure that the results were not donor specific. Similar medium lacking conditioning by human MSC was collected as control medium (CTL-CM)[50]. Conditioned growth medium was concentrated tenfold through YM-3 centrifugal filter devices with YM-100 (100,000 MW) devices (Millipore, Billerica, MA). This 100-kDa fraction was termed $MSC\text{-}CM_{100kDa}$. Protein concentrations were estimated using the BCA Protein Assay Kit (Pierce, Rockford, IL), and 0.5 mg protein was used for cell culture and *in vivo* studies. Recombinant HGF, cMet and anti-HGF were purchased from R&D Systems (Minneapolis, MN). Two doses of recombinant HGF (50 ng and 100 ng) were injected intravenously on day 14 at peak disease every other day for a total of three injections. For cMet antibody treatment, animals were injected 24 h before treatment. Conditioned medium was incubated with function-blocking anti-HGF for 1 h before use. In culture, HGF was used at 45 ng per 2×10^5 cells and anti-cMet at 50 ng per 2×10^5 cells, added 1 h before HGF.

Western blot. Conditioned-medium proteins were separated on 10% SDS-polyacrylamide gels, transferred to a polyvinylidene difluoride membrane, and incubated with monoclonal primary antibodies to HGF (Cell Signaling Technology, Beverly, MA) and HRP-conjugated secondary antibodies. Visualization was performed with an enhanced chemiluminescence system (ECL, GE Healthcare Biosciences, Piscataway, NJ) according to the manufacturer's instructions.

Neuropathology. Sections (4% PFA fixed) were stained with hematoxylin and eosin (H&E) for detection of inflammatory infiltrates and luxol fast blue (LFB) for myelin detection. For electron microscopy, animals were perfused with 2.5% glutaraldehyde. CNS tissues were postfixed in 1% osmium tetroxide for 1 h, dehydrated and embedded in epoxy resin. One-micrometer epoxy sections were stained with toluidine blue and examined by light microscopy. For EM, thin sections were stained with uranyl acetate and lead citrate, and examined in a Joel 100CX microscope at 80 kV. For LFB, H&E and toluidine blue analysis, three different animals were assayed with at least 16 sections per animal. Quantification of the proportion of myelinated and unmyelinated axons was taken from multiple sections at least 2 different spinal cord regions from 2 animals. G ratios were determined by analysis of at least 200 axons in each condition. For analysis of lesion load, the data were obtained from 10 sections taken from 3 different animals of each control and HGF-treated EAE. Data was collected using ImageJ, and the units represent $cm^2 \pm$ s.d. Sample sizes were determined based on power estimates. Lesions were identified as shadow areas in LFB stained sections. Lesion volumes were calculated from serial sections through the lesion on the basis of the equation for the volume of an elliptical cone ($V = (\pi/3)abh$) and location of the lesion midpoint. All images were taken by an investigator blinded to the treatment of the individual animals.

Neural cell cultures. Neurosphere cultures were prepared from newborn mouse cortex and adult SVZ and grown in 10 ng ml^{-1} epidermal growth factor. Second-passage neurospheres were dissociated and plated at 2×10^5 cells per coverslip in the absence or presence of whole (MSC-CM) or fractioned ($MSC\text{-}CM_{100\ kDa}$), recombinant HGF ± anti-cMet. (1:50; Santa Cruz Biotechnology, Santa Cruz, CA) for 3 d before analyses. Cells were labeled with antibodies to Nestin (rat-401, Developmental Studies Hybridoma Bank, Iowa City, IA, cat. no. Rat 401), A2B5, O4, β-tubulin III (Sigma-Aldrich, St. Louis, MO (cat. no. T8660) and GFAP (R&D Systems, Minneapolis, MN, Catzo334). The proportion of positive cells was determined in three randomly selected areas per coverslip in at least three separate experiments derived from three independent neurosphere preparations. Data were assessed by independent *t*-test.

To determine the effects of $MSC\text{-}CM_{100kDa}$ and HGF on the migration of neurosphere derived cells, neurospheres were grown for 14 d and replated on poly-L-lysine–coated coverslips in the presence of $MSC\text{-}CM_{100kDa}$, $MSC\text{-}CM_{100kDa}$ + anti-cMet, $MSC\text{-}CM_{100kDa}$ + anti-HGF and HGF + anti-cMet. Cells were allowed to migrate for 24 h and the preparations fixed with cold methanol and processed for immunohistochemistry as above. Cerebellar slice cultures were established from 300-µm sagittal slices of P9 cerebellum cut on a Leica Vibratome. Slices were grown for 3 d in DMEM/BME with N2 and PDGF-AA (20 ng ml^{-1}) before being switched to media containing 15% horse serum. Slices were treated with lysolecithin (LPC, Sigma) at a final concentration of 0.5 mg ml^{-1} for 16 h, rinsed and then incubated in either control medium or control medium containing 50 ng ml^{-1} HGF for 3 to 7 d. Oligodendrocyte ensheathment was assayed by MBP expression (Covance, SMI99, Invitrogen Alexa 594). Cortical slices were treated similar but obtained from coronal sections of P4 brain and grown for 4 d before LPC treatment.

ELISPOT assay for $MOG_{35–55}$-specific $CD4^+$ T cells in the CNS. Cells were isolated from the spinal cords of animals with EAE following gross manual disruption, filtered, washed and counted. ELISPOT plates (Millipore, Billerica, MA) were coated with IFN-γ antibody (eBiosciences, San Diego, CA, no. AN-18), anti–IL-10 (eBiosciences, cat. no. JES5-2A5) or anti–IL-17 (eBiosciences, cat. no. 88-7876-21) overnight. Cells were stimulated with medium alone or with 10 µg ml^{-1} autoantigen. Subsequently, biotinylated anti–IFN-γ (eBiosciences no. R4-A2), anti–IL-10 or anti–IL-17 (eBiosciences; see above) was added, followed by streptavidin-HRP (Mabtech cat. no. 3310-9) and developed with TMB ELISPOT substrate (Carl Zeiss Vision, Hallbergmoos, Germany). Spots were counted by AID ELISPOT plate reader version 4.0. Individuals were designated as responders if the numbers of spots in the presence or absence of HGF or HGF plus anti-cMet were significantly altered (*t*-test, $P < 0.05$) from controls and the frequency of myelin reactive $CD4^+$ cells calculated .

Cytokines analysis. IL-17, IFN-γ, TNF-α, IL-2 (eBiosciences, no. BVD624G2), IL-10 and IL-4 were analyzed with the Qiagen LiquiChip System (BioChipNet, Reutlingen, Germany) using anti-mouse monoclonal antibodies (see above) with supernatant samples and standards in duplicate. Data represent mean ± s.d. assayed by *t*-test ($n = 3$). Biotinylated secondary antibodies were added followed by streptavidin–horseradish peroxidase and peroxide–chromogen substrate following the manufacturer's instructions.

49. Kerstetter, A.E., Padovani-Claudio, D.A., Bai, L. & Miller, R.H. Inhibition of CXCR2 signaling promotes recovery in models of multiple sclerosis. *Exp. Neurol.* **220**, 44–56 (2009).
50. Lennon, D.P. & Caplan, A.I. Isolation of human marrow-derived mesenchymal stem cells. *Exp. Hematol.* **34**, 1604–1605 (2006).

doi:10.1038/nn.3109